II.I.6 Use of Biological Materials and Biologically Inspired Materials for H_2 Catalysis*

John W. Peters (Primary Contact),
Trevor Douglas, Mark Young
Chemistry and Biochemistry Building
Montana State University
Bozeman, MT 59717
Phone: (406) 994-7211; Fax: (406) 994-7212
E-mail: John.Peters@chemistry.montana.edu

DOE Technology Development Manager:
Roxanne Garland
Phone: (202) 586-7260; Fax: (202) 586-2373
E-mail: Roxanne.Garland@ee.doe.gov

DOE Project Officer: Lea Yancey
Phone: (303) 275-4944; Fax: (303) 275-4753
E-mail: Lea.Yancey@go.doe.gov

Contract Number: DE-FC36-06GO8606

Project Start Date: August 1, 2006
Project End Date: December 31, 2009

*Congressionally directed project

Objectives

- Optimize the hydrogenase stability and electron transfer.
- Optimize the semiconductor nano-particle catalysis, oxygen scavenging, and electron transfer properties of protein nano-cages.
- Gel/matrix immobilization and composite formulation of nano-materials and hydrogenase.
- Device fabrication for H_2 production.

Technical Barriers

This project addresses the following technical barriers from the Hydrogen Production section of the Hydrogen, Fuel Cells and Infrastructure Technologies Program Multi-Year Research, Development and Demonstration Plan:

(AL) Light Utilization Efficiency

(AM) Rate of Hydrogen Production

(AN) Hydrogen Re-oxidation

(AP) Systems Engineering

Technical Targets

Photoelectrochemical Hydrogen Production

Protein-Based Hydrogen Production Materials/Devices:

- This project is conducting fundamental studies of hydrogenase enzymes and biomimetic nanoparticle mimics and their incorporation into durable materials. Insights gained from these studies will be applied toward the design and synthesis of hydrogen production materials/devices to probe specific metrics for competitive evaluation including:
  - Shelf life of the hydrogen catalyst.
  - Longevity of catalyst under sustained hydrogen production.
  - Thermal stability.

Accomplishments

- Demonstrated that hydrogenase enzymes can be encapsulated within silica gel matrices for enhanced ease of fabrication, without loss of activity, and with some stabilization towards degradation.
- Demonstrated that hydrogen production activity of encapsulated hydrogenases is sensitive to pH.
- Demonstrated that encapsulated hydrogenase materials can be reused and recycled.
- Demonstrated that electroactive gel matrices (polyviologen and viologen doped silica gels) can be manipulated to effect hydrogen production activity.
- Demonstrated efficient hydrogen production with noble metal nanoparticles synthesized using protein cage architectures. Hydrogen production rates are competitive with enzyme catalyzed (hydrogenase) reactions.
- Discovered that hydrogen production can be achieved with pure noble metal and noble metal alloy composite nanoparticles (2009).
- Demonstrated size dependent catalytic efficiency on a range of nanoparticle constrained nanoparticles and demonstrated that nanoparticle size affect catalytic activity (2009).
- Demonstrated thermal stability of both hydrogenase enzymes and synthetic biomimetic catalyst composites up to 90°C with hydrogen production.
- Determined a potential structural basis for the observed enhanced thermal stability observed for the [NiFe]-hydrogenase from *Thiocapsa roseopersicina* (2009).

- Demonstrated sustained hydrogen production for up to 2 hrs (synthetic catalyst) when coupled to light harvesting system, which meets the 2013 target for continuous photoproduction.
- Demonstrated construction of protein cage nanoparticles with integrated $Ru(phen)_3$ light-harvesting photocatalyst.
- Demonstrated mediator-less light harvesting and electron transfer to protein caged Pt nanoparticles.
- Demonstrated increased O_2 tolerance for hydrogenase enzymes that meet the 2013 target (10 min).
- Demonstrated that the addition of carbon nanotubes can enhance activity of hydrogenase encapsulated in sol gels (2009).
- Demonstrated that sol gel encapsulation of hydrogenases can be optimized with the addition of carbon nanotubes and polyethylene glycol to yield activities equivalent to the maximum activities observed in solution (2009).

Introduction

There is significant interest in the use of hydrogen gas as an alternative fuel for the rapidly evolving hydrogen fuel cell technology. The practicality of the increased use of hydrogen fuel cell technologies is dependent on the ability to produce stores of hydrogen gas in an efficient, economically feasible, and environmentally sound manner. The development of catalysts for the production of hydrogen gas efficiently from a renewable source is of paramount importance.

Biological production of hydrogen is likely to play a key role in the emerging hydrogen economy. In particular, a group of enzymes, hydrogenases (H_2ases), have attracted a great deal of attention because of their ability to efficiently catalyze the reversible reduction of protons to form hydrogen in the absence of Nobel metals. The catalytic site of H_2ases enzymes consists of unique biological metal clusters (Fe or NiFe) stabilized by carbon monoxide and cyanide ligands.

Approach

Using approaches previously described we have optimized the synthesis of biomimetic catalyst systems by encapsulation of reduced metal nanoparticles (Pd, Pt, Fe, Co, and Ni) within engineered protein architectures to mimic the activity and buried active sites of H_2ases enzymes. These materials, along with H_2ases enzymes themselves, have been incorporated into a variety of polymer matrices for efficient hydrogen production and catalyst stabilization.

Overall we are developing composite materials that consist of hydrogen-generating catalytic materials (either hydrogen enzymes or Pd, Pt, Fe, Co, Ni or mixed metal mimics) coupled to photocatalytic materials (for utilization of light energy) or exogenous reducing agents (chemical or electrochemical). These composite materials represent a practical sustainable means of generating hydrogen gas from fully renewable sources. Our most recent efforts have focused on the characterization of H_2ases stability and the further stabilization of H_2ases enzymes to promote increased durability for their use in materials and hydrogen production devices. In addition, using biomimetic approaches enzyme mimics have been synthesized using a range of metal-based nano-materials, including Pt, Pd, Fe_2O_3, Co_3O_4) that mimic the catalytic properties of the enzyme but can be mass produced more readily and have desirable features in the context of durability and oxygen tolerance.

Results

One of the research thrusts is in the area of biomimetic protein cage templating of nanoparticle synthesis. Protein cages provide a scaffold for composite materials synthesis where the spatial arrangement of small molecules (such as light harvesting systems) and encapsulated nanoparticles is optimized for purposes such as light-driven hydrogen production. The long-term goal of using protein assemblies for energy conversion requires that we need to understand the range of chemistries tolerated by the protein and work to enhance the overall stability and fidelity of the synthetic reactions to which we subject them. The second research thrust focuses on hydrogenase enzymes that are highly evolved biological hydrogen production catalysts. Hydrogenase have tremendous promise to be utilized for hydrogen production in living and bimimetic systems. Our work is based mainly in determining the structural basis for stability of those hydrogenases that naturally have enhanced stability and developing mechanisms to be able to treat hydrogenases as heterogeneous catalysis in materials while maintaining their optimal catalytic efficiencies.

1. Removing the electron transfer mediator: direct light harvesting and catalyst turnover.

To improve the effective number of turnovers the photocatalysts can undergo before significant reaction rate decay is observed we have taken a two-pronged approach. First we have designed and constructed a high lux light emitting diode (LED) light source with an average output wavelength of 460 nm. This wavelength is well suited for both the $[Ru(bpy)_3]Cl_2$ and $[Ir(ppy)_2(bpy)]PF_6$ light harvesting catalysts we have employed. The use of this light source over others (i.e. Xe lamps) will improve photocatalyst lifetime by

only providing photons near the desired metal to ligand charge transfer energy. Preliminary results indicate that the initial reaction rate may be slightly depressed compared to the Xe lamp, but that the overall production is equivalent in the $[Ru(bpy)_3]Cl_2$ system and improved in the $[Ir(ppy)_2(bpy)]PF_6$ system (Figure 1). We are currently working to make a protein-photosensitizer construct using a genetically modified small heat shock protein (G41-sHsp) whose introduced internal cysteine is labeled with either $[Ru(bpy)_2(Iphen)]^{2+}$ or $[Ir(ppy)_2(Iphen)]^{+}$, where Iphen is 5-iodoacetamido-1,10-phenanthroline. We have successfully synthesized both photosensitizer constructs and have successfully labeled G41C-sHsp with both sensitizers with the labeling for the ruthenium compound optimized for a single sensitizer per a subunit. Using the ruthenium complex labeled G41C-sHsp we have mineralized Pt^0 inside the protein cage using the conditions we previously published for sHsp. Using this labeled and mineralized protein in a qualitative hydrogen production test resulted in some hydrogen production indicating that the ruthenium complex retains its ability to behave as a photosensitizer for hydrogen production even after being attached to the protein. This effort will determine the overall efficiency of a mediator-less system with direct electron transfer between light harvesting and H^+ reduction catalyst [Pub. 2]. Cage stabilization and covalent incorporation of light harvesting molecules into protein cage framework.

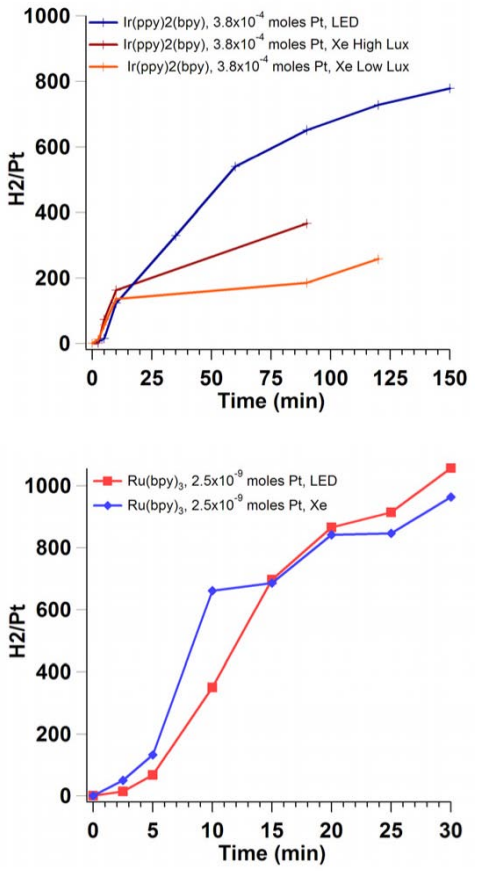

FIGURE 1. Light source dependent hydrogen production using either an LED or Xe light source with $Ru(bpy)_3^{2+}$ (bottom) or $Ir(ppy)_2bpy^+$ (top) as the light harvesting system in conjunction with cage-Pt nanoparticles.

We have exploited the small heat shock protein (Hsp) from *Methanococcus jannaschii* as a platform for encapsulation of Pt nanoparticle for hydrogen production. To expand the usefulness of this system we have enhanced the chemical and thermal stability of the Hsp protein cage. We have genetically engineered an Hsp mutant, HspE102C, in which the residue 102 is substituted from glutamic acid to cysteine. This cysteine is now available as a chemically-specific reaction site on the protein cage. Since the residue 102 is located around three fold axis of the Hsp, this cysteine residue is expected to be utilized as a site to cross-link three subunits around the axis together so that the cross-linked cage would become more robust. We have conjugated 5-iodoacetamido-1, 10 phenanthroline (I-Phen) on the cysteine 102, followed by coordination of Fe^{2+} with the three Phen around the three fold axis of the cage. The HspE102C cage cross-linked with the $[Fe(Phen)_3]^{2+}$ complex maintained its original size (~13 nm) even after heat treatment at 80°C for 20 min, whereas the "uncross-linked" HspE102C cage aggregated after heating at 65°C for 10 min. This indicates the $[Fe(Phen)_3]^{2+}$ complex formed between subunits could work as a "linker" among the three subunits and stabilize the cage structure. Furthermore, since $[Fe(Phen)_3]^{2+}$ complex is structurally similar to well know photosensitizer $[Ru(Bpy)_3]^{2+}$ and $[Ir(Bpy)_3]^{+}$ for H_2 production catalyzed by Pt, it would be possible to impart light harvesting capability and higher stability to the Hsp cage simultaneously by using a iodoacetamido derivative of these photosensitizer as a cross-linker at the 3-fold axis of the Hsp102C.

3. Monitoring and controlling particle size growth of Pt nanoparticles.

We have focused on developing more efficient Pt nanoparticle formation within our protein cages. Previously, we constructed genetically modified LiDps and chemically attached metal binding ligands (phenanthroline) to achieve directed Pt nanoparticle formation within LiDps. Now, we have successively monitored Pt ion binding and Pt nanocluster formation individually using mass spectrometry (MS). We have also developed a serial growth method and monitored nanocluster growth using MS and transmission electron microscopy (TEM).

Genetically modified (S138C) LiDps was prepared and incubated with a small amount of Pt ions (50Pt(II)/cage) overnight. In order to make a Pt seed within LiDps, Pt treated LiDps were reduced with

equivalent amount of $NaBH_4$ and dialyzed overnight to remove unreacted Pt. Subsequent growth of Pt nanoparticle within LiDps was induced by introducing 100 or 200 Pt(II)/cage with equivalent amount of $NaBH_4$ at 65°C for 30 min. Reaction products were analyzed by size exclusion chromatography and elution profiles clearly showed co-elution of protein cages and Pt nanoparticle. Electron micrographs of negative stained Pt-mineralized LiDps revealed an intact cage-like structure and distinct particles were observed with additional 200 Pt(II)/cage without staining. To determine the absolute number of Pt atoms of naoparticles formed within LiDps, we performed noncovalent mass spectrometry analyses of Pt treated samples. MS analyses indicated seeding step (50Pt(II)/cage) induced formation of nanocluster with 37 Pt atoms within LiDps on average. Further high temperature syntheses with additional 100 and 200 Pt(II)/cage produced Pt nanoparticles containing 168 and 202 Pt atoms within LiDps on average. This approach, seeding and subsequent high temperature, can easily apply to other protein cage systems to improve the efficiency of encapsulation of metal nanoparticles.

4. Molecular conjugation and measurement of electron conduction.

A derivative of the transition metal complex $Ru(bpy)_3^{2+}$ was conjugated to a mutant (G41C) of Hsp. G41C is a genetic construct that presents cysteines on its interior surface. G41C provided a robust nanoplatform that allowed relatively high loading of an isothiocyanate derivative of $Ru(bpy)_3phen^{2+}$ (Figure 2a) onto the cage via conjugation to primary amines. The absorbance from the $Ru(bpy)_3phen^{2+}$ at 450 nm was prominent in the cage preparations (Figure 2b). The ratio of $Ru(bpy)_3phen^{2+}$ to monomeric subunit was estimated as 2.5 based on the ultraviolet-visible (UV-VIS) absorbance and protein content determined by a bicinchoninic acid assay. This translates to 60 $Ru(bpy)_3phen^{2+}$ per cage. The functionalized cage appears as intact 12 diameter particles on TEM grids (Figure 2c). It forms films on silicon wafers coated with poly-L-lysine visualized using field emission scanning electron microscopy (Figure 2d). According to particle counts acquired from these images the fractional area coverage is 0.56, which conforms to that expected from the random sequential adsorption (RSA) model (0.55).

The G41C $Ru(bpy)_3phen^{2+}$ conjugate was adsorbed to an indium tin oxide (ITO) electrode. We found that an ITO electrode provided the most favorable background for the expected potential range of the $Ru(bpy)_3phen^{2+}$ redox couple ($E_o = 1.26$). The red fluorescence from the $Ru(bpy)_3phen^{2+}$ was evident in images acquired using epi-fluorescence microscopy (Figure 2e). The red hue appears slightly less intense than that of the conjugate adsorbed to poly-L-lysine coated plastic microtiter plate wells (Figure 2e, inset).

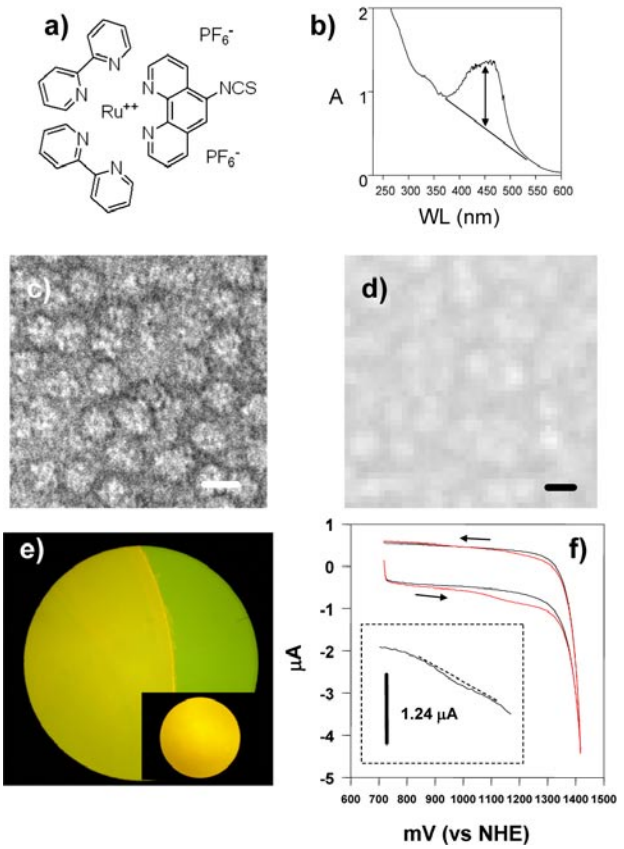

FIGURE 2. Electron transport from a redox couple conjugated to a protein cage. a) $Ru(bpy)_3phen\text{-}SCN^{2+}$ conjugation agent; b) UV-VIS spectrum of the functionalized protein cage (G41C $Ru(bpy)_3phen\text{-}SCN^{2+}$ c) TEM image of G41C $Ru(bpy)_3phen\text{-}SCN^{2+}$ (scale, 12 nm); d) FE SEM image of G41C G2.5 $Ru(bpy)_3^{2+}$ on poly-L-lysine coated silicon (scale, 12 nm); e) epi-fluorescent image of G41C $Ru(bpy)_3phen\text{-}SCN^{2+}$ adsorbed to an ITO electrode surface from a drop; green region is the clean ITO surface; inset is an image of G41C $Ru(bpy)_3phen\text{-}SCN^{2+}$ adsorbed to poly-L-lysine coated plastic well; f) Cyclic voltammogram trace of buffer (black) and ITO electrode with a film of G41C $Ru(bpy)_3phen\text{-}SCN^{2+}$ (red); inset is detail of the oxidation curve.

This difference in fluorescence perceived by the eye is validated by the difference in the ratios of the red channel to the total luminescence, which is less for the conjugate adsorbed on the ITO surface (1.15) than for the poly-L-lysine coated surface (1.25). Cyclic voltammograms (CVs) were acquired from the adsorbed film (Figure 2f). There were clear differences between the CV of the buffer (100 mM sodium acetate, pH 5.7) and the adsorbed film. Based on the interpretation that the feature in the positive sweep originates from the oxidation current, the area under this feature yields the total electrons transferred from the $Ru(bpy)_3phen^{2+}$ conjugated to G41C in the film. The inset shows that this area is actually quite small. Assuming that the adsorbed amount of G41C in the film conforms to the RSA model, this quantity of electrons would be expected to be transferred if only one of the $Ru(bpy)_3phen^{2+}$

per cage were in electrical contact with the electrode surface. The height of the oxidation curve expected if electrons from all the $Ru(bpy)_3^{2+}$ conjugated to the cage in the film were transferred is shown by the vertical bar in the inset.

These results suggest strongly that the Hsp G41C is fairly insulating and that catalystic H_2 production probably requires diffusion of mediator through the protein shell to contact the encapsulated nanoparticle catalyst. The estimate of $Ru(bpy)_3phen^{2+}$ in electrical contact with the electrode depends directly on the estimation of the adsorbed surface coverage and thus could be low. Based on the differences in fluorescence from the adsorbed films mentioned above a rough estimate suggests that perhaps the coverage on the ITO electrode is 50% that on the poly-L-lysine coated surfaces. However, the difference between the expected height of the oxidation curve if all electrons from the film were collected, and the actual height, is still striking.

5. Investigation and optimization conditions for developing composite materials based on encapsulation of hydrogenase and multiwall carbon nanotubes into sol-gel.

During the reporting period we have been continuing our work on the optimization conditions for hydrogen production by the *T. roseopersicina* hydrogenase encapsulated into sol-gel. We have shown that hydrogenase encapsulated into sol-gel remains active in presence of carbon nanotubes. The results of these experiments provide the important information about the properties of composite materials composed of silica-gel, carbon nanotubes and encapsulated hydrogenases indicating that carbon nanotubes have high efficiency to conduct electron flow from electron donor/acceptor to hydrogenase in silica-gel. Different type of carbon nanotubes (single- or multi-wall nanotubes) has been developed for this application. The results of our experiments with single- or multi-wall carbon nanotubes show no difference in the activity of hydrogenase encapsulated into sol gel in presence of 4 mM methyl viologen (MV) as an electron carrier.

We have shown previously that increasing the concentration of nanotubes increases the hydrogen production by the hydrogenase in presence of MV. In this study we for the first time are showing the direct transport of electrons through multiwall carbon nanotubes to the hydrogenase without using MV as an electron carrier (Figure 3). Addition of MV increases the hydrogen evolution by encapsulated hydrogenase. The hydrogen production by this system was significantly dependent on the pH of the reaction mixture and was 5 times higher at pH 5.5 in compare to pH 8.0. It has been shown that activity of hydrogenase in solution also dependent on pH and was ~2 times higher at pH 5.5 than at pH 8.0 (Figure 3) [1].

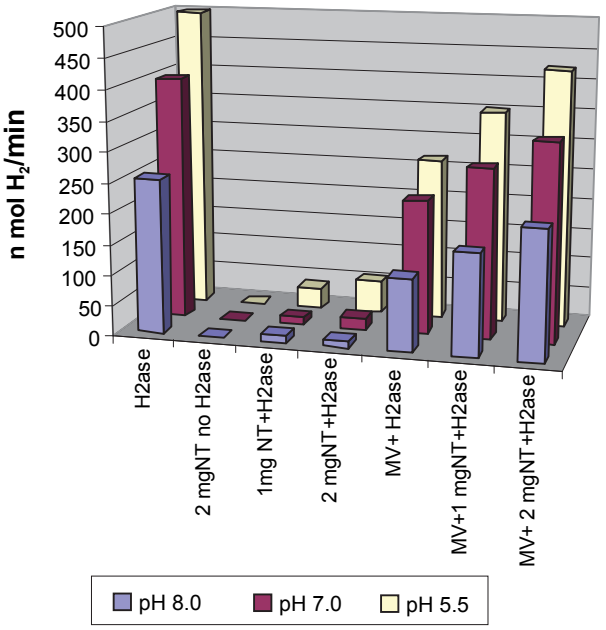

FIGURE 3. Effect of pH and concentration of multi-wall carbon nanotubes on the hydrogen production by encapsulated hydrogenase.

We have examined the effect of the addition of polyethylene glycol (PEG) to gels on the activity of *T. roseopersicina* hydrogenase at different pH. Previously it has been shown that the addition of PEG to sol gels can modulate the pore size of the gels and have significant effects on mass transfer [2]. The reaction mixture consists of 50 mM phosphate buffer pH 5.5, 7.0 and 8.0 and polymerized sol gel. The sol gel was prepared from tetramethoxy silane with the addition of different concentrations of PEG with molecular weight 400 (PEG 400) and/or multiwall nanotubes in presence of 2 or 4 mM methyl viologen. Sol gel was polymerized during 10 min with the addition of an equal volume of 0.8 mg/ml hydrogenase in 50 mM phosphate buffer pH 7.5. The results of our experiments show that increasing PEG concentration from 0% to 20% increases the activity of hydrogenase, whereas 40% PEG inhibited the hydrogen production by encapsulated hydrogenase. The addition of PEG did not influence on the hydrogenase activity in solution. The results of our experiments show that optimum conditions for the development of composite material based on encapsulation of hydrogenase and nanotubes consist of 20% PEG and 2 mg nanotubes and 4 mM methyl viologen at pH 5.5. Under these optimal conditions for encapsulation, hydrogenase activities equivalent to the maximum activities in solution were observed.

6. Structural analysis of the [NiFe]-hydrogenase from Thiocapsa roseopersicina.

During the current grant period we have been working on structural characterization of *T.*

roseopersicina [NiFe]-hydrogenase. It has been shown that this hydrogenase is stable to high temperature and oxygen. These properties make this enzyme attractive in the application for hydrogen producing materials. We have previously reported our progress toward the structure of the [NiFe]-hydrogenase from *T. roseopersicina* using cryo electron reconstruction experiments. It has been shown that at high protein concentration (~10 mg/ml) this enzyme forms the supermolecular complex [3]. The specific interactions that stabilize this structure are likely significant to the overall stability of this enzyme and the structure of this assembly is of significant interest in order to identified these factors. We have determined the low resolution structure of hydrogenase assembly using cryo-electron microscopy revealing the supermolecular complex consists of six dimers, organized in D3 hexamer and that the C-terminus of the small subunit of each dimer are involved in key interactions that stabilize the complex. We have also obtained crystals of this hydrogenase and have determined the structure by multiple isomorphous replacement and anomalous scattering methods. Figure 4 shows images of electron density map, obtain after phase extension, using CCP4 program presented in Figure 4. These results correlated with the CryoEM reconstruction images, showing 3-fold (Figure 4 (A, C), 2-fold (Figure 4 C, D) and inner core structure of *T. roseopersicina* hydrogenase supermoleular complex. The secondary structure elements are clearly visible in these maps and we have started to build the structure into these maps taking advantage of the known structure of the [NiFe]-hydrogenase from *D. gigas* as a starting model.

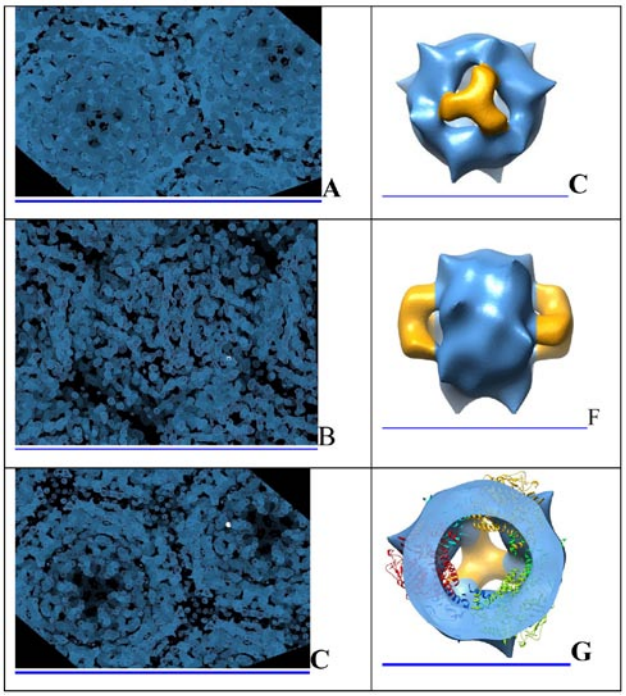

FIGURE 4. Structural characterization of hydrogenase from *T. roseopersicina*. A, B, C are 4.5 Å MIR phased map, D, F, G Cryo electron microscopy reconstruction model. A and C represented 3-fold symmetry, B and F – 2 fold symmetry, C and G inner core of hexamer structure.

Conclusions and Future Directions

The project has laid a firm groundwork for the use of H_2ases and synthetic mimetics in hydrogen producing materials. The project demonstrates that materials can be generated that have reasonable shelf lives and high catalytic capabilities. We have systematically developed strategies to adapt both H_2ases and synthetic mimetics for use in prototype hydrogen production devices. The salient advancements in the previous year of funding include:

- Major advancements were made in the area of synthesis of noble metal and noble metal alloy catalytic nanoparticles and the incorporation of nanoparticles and H_2ases into electroactive gels and onto surfaces.
- Tools have been developed to advance biomimetic/biohybrid device design and fabrication.
- Twenty two presentations and publications and one patent pending.

The remainder of the project will focus on preparing manuscripts for publication and as future directions we will focus mainly on the direct attachment of catalysts and the attachment of gel encapsulated catalysts to electrode surfaces to directly assess the efficacy of our novel materials for use in devices.

References

1. Zorin, N.A.; Dimon, B.; Gagnon, J.; Gaillard, J.; Carrier, P.; Vignais, P.M. Inhibition by iodoacetamide and acetylene of the H-D exchange reaction catalyzed by Thiocapsa roseopersicina hydrogenase – pH dependence Eur J Biochem 1996, 241, (2), 675-81.

2. Sherman, M.B.; Orlova, E.V.; Smirnova, E.A.; Hovmoller, S.; Zorin, N.A. Three-dimensional structure of the nickel-containing hydrogenase from Thiocapsa roseopersicina. J Bacteriol 1991, 173, (8), 2576-80.

3. Sato, S.; Murakata, T.; Suzuki, T.; Ohgawara, T. Control of pore size distribution of silica gel through sol-gel process using water soluble polymers. J. Mater. Sci. 1990, 25, 4880-4885.

Patents Issued

1. PCT/US06/018,900 – Composite nanomaterials for photocatalytic hydrogen production and methods of their use (May 16, 2006).

FY 2009 Publications/Presentations

John Peters

Publications

1. M.C. Posewitz, D.M. Mulder, and J.W. Peters "New Frontiers Into Hydrogenase Structure and Biosynthesis" *Curr. Chem Biol.* 2, 178-199 (2008).

2. J.W. Peters "Carbon monoxide and Cyanide Ligands in the Active Site of [FeFe] Hydrogenases" in *Met. Ions Life Sci.* (2009), (Metal-Carbon Bonds in Enzymes and Cofactors).

Trevor Douglas

Publications

1. S. Kang, C.C. Jolley, L.O. Liepold, M. Young, and T. Douglas, "From Metal Binding to Core Formation; Monitoring Biomimetic Iron Oxide Synthesis within Protein Cages using Mass Spectrometry", *Angew. Chemie.* (2009) *48, 1-6.*

2. Z. Varpness, P. Suci, M. Young, T. Douglas "$^{1}O_2$ production in Hsp" *Chem Commun* (2009) *3726–3728.*

Presentations

1. Astrobiology Center, University of Colorado Boulder, Nov 12, 2008.

2. "Protein Cage Architectures: templates for molecular and materials science" Dec 2008 – Hunter College NY, Department of Chemistry.

3. "Viral Capsids And Other Self-Assembled Protein Cage Architectures: Supramolecular. Templates For Molecular And Materials Encapsulation" February 5, 2009 - Harvard University, Department of Chemistry.

4. "Capsids for synthetic encapsulation: polymers, molecules and nanosolids." Invited speaker at Gordon Research Conference on Physical Virology, Feb 15–20, 2009, Galveston Texas.

5. "Self-Assembled Protein cage Architectures – Supramolecular Templates for Nanomaterials Synthesis" April 2009 Invited Speaker at 12th International Seminar on Inclusion Compounds, Stellenbosch, South Africa.

6. "Self-Assembled Protein cage Architectures – Supramolecular Templates for Nanomaterials Synthesis" April 2009 – University of Minnesota Department of Chemistry.